



Multi-frequency VLBA Polarimetry of GPS Quasar OQ172

Liu, Yi

Purple Mountain Observatory, CAS



Outline

1. Motivation

2. Observation

3. Results

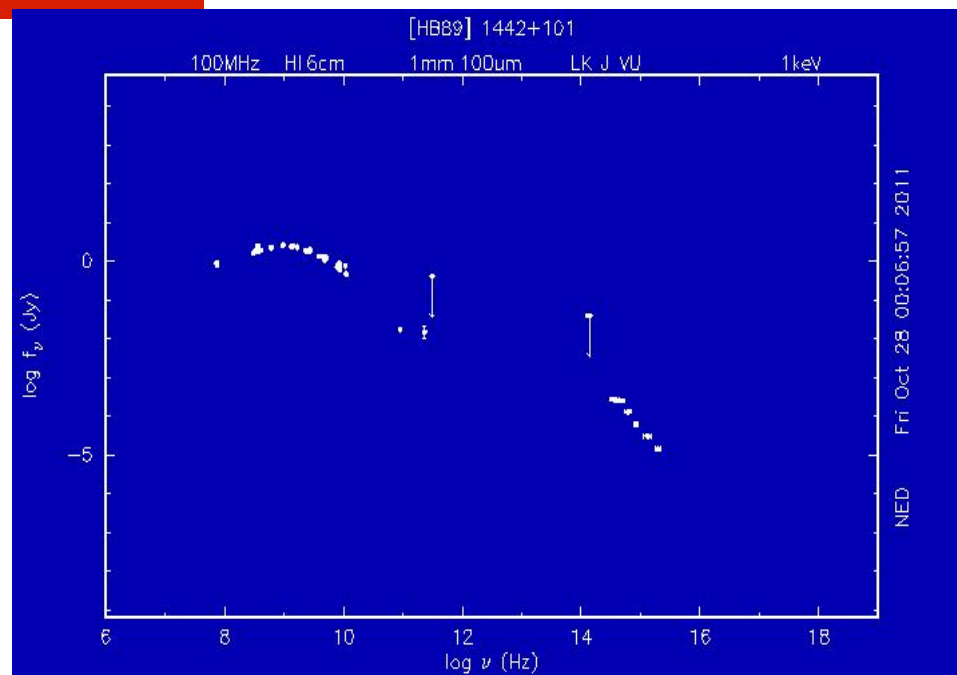
4. Conclusion



Information of GPS OQ172

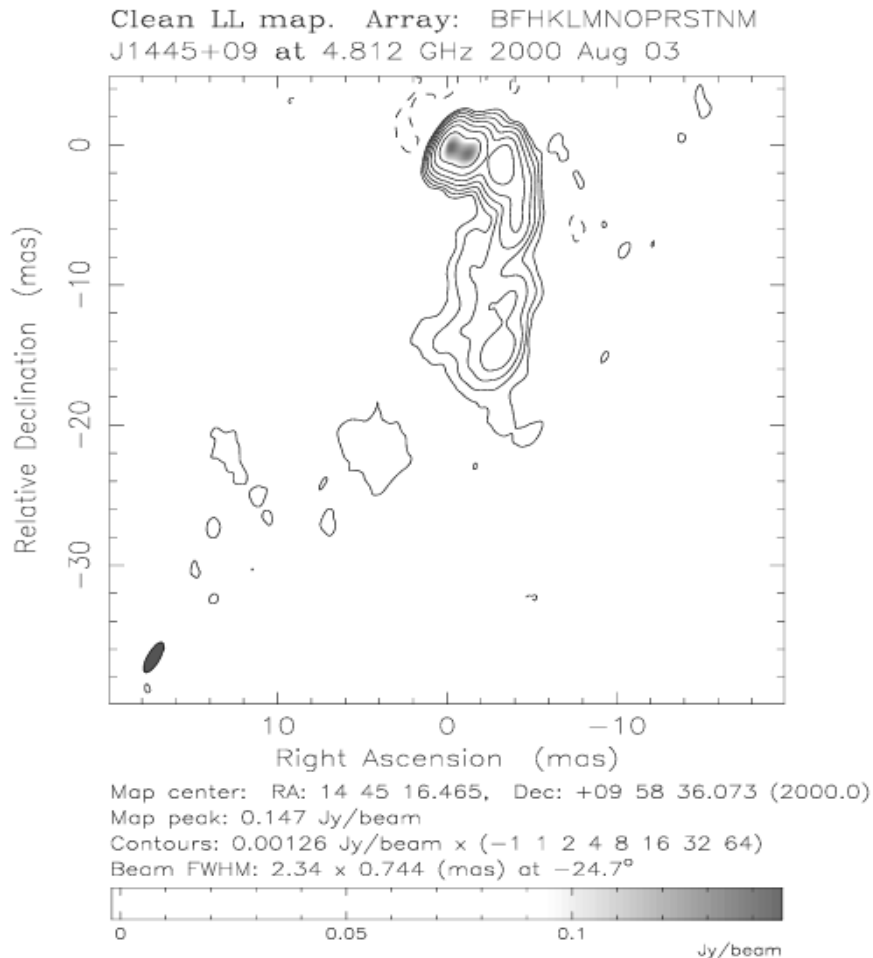
GPS Quasar: GHz-Peaked Spectrum (GPS) radio sources are characterized by their compact size ($L < \sim 100\text{pc}$) and convex spectrum peaked at $\sim 0.5\text{-}10\text{ GHz}$ observed frequencies (O' Dea et al. 1991).

At the peak turnover frequency, the optically thin radio synchrotron radiation transitions to optically thick emission, though there is still debate over whether this is caused by Synchrotron Self-Absorption (SSA) or Free-Free Absorption (FFA) (O' Dea 1998).





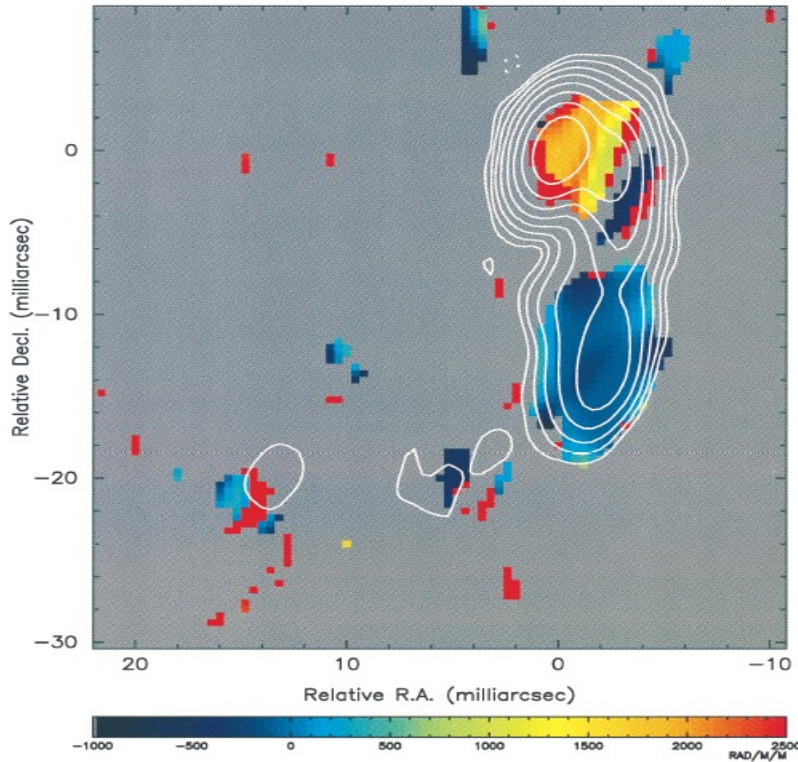
VSOP 5GHz image



-- GPS quasars appear as core-jet structure, in line with AGN unified schemes

- no kpc-scale radio structure
- a compact N-S elongation
- the jet suffers a large bend at ~ 3 mas from the northern-most component

UDOMPRASERT et al. 1997



→ high RM 20,000 rad m⁻² in the rest frame, and 100 rad m⁻², 10mas from nucleus

→ one of the highest among ~20 known high-RM sources

H β FWHM 3,700 kms⁻¹

[O III] FWHM 2,200 kms⁻¹

NIR spectrum, (Hirst et al. 2003)



VLBA OBSERVATION

We propose L,S,C,X,U-band VLBA polarimetry to investigate the following inter-related questions about the unusual circumnuclear environment of OQ172, as seen in highly-redshifted mm-wave emission from 6-70 GHz in the source rest frame:

- What is the magnetic field topology?
- What is the GPS absorption mechanism?
- Why is the RM extremely high, and the inner jet depolarized?
- Why is the jet strongly bent and curved, and how do physical properties vary along its length?
- Where is the VLBI core?



VLBA OBSERVATION

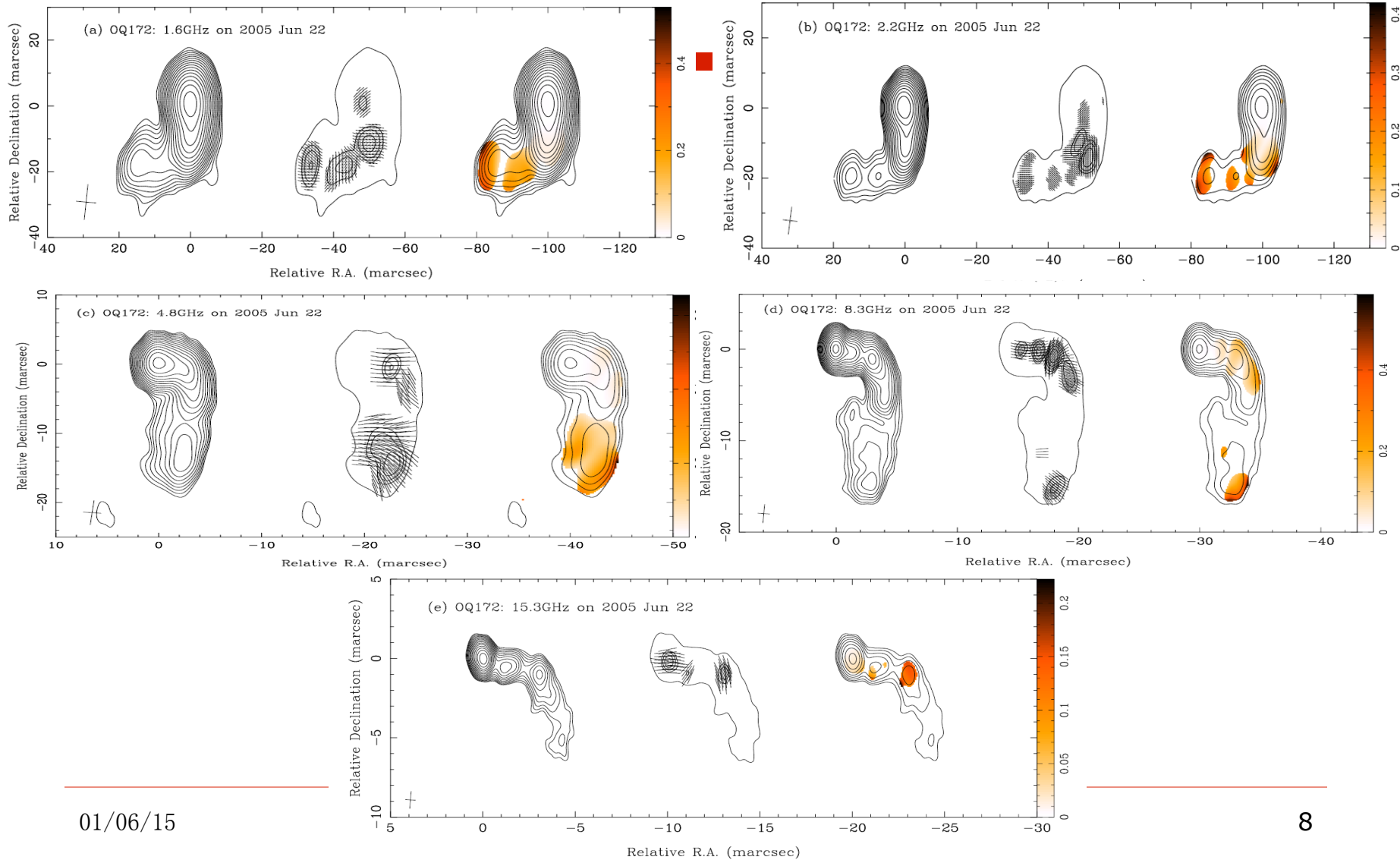
Sources

OQ172 (Target)	OQ208 D-term	3C286 EVPA(1, 2, 5GHz)	3C279 EVPA (8, 15GHz)
-------------------	-----------------	---------------------------	--------------------------

Observation Frequency (GHz)				BW	Scan	Time (min)
1.412	1.502	1.592	1.683	8MHz	24	72
2.166	2.211	2.256	2.302	8MHz	24	72
4.630	4.770	4.910	5.051	8MHz	24	102
8.116	8.196	8.396	8.537	8MHz	23	134
15.140	15.220	15.421	15.561	8MHz	34	191



Total intensity distribution and Polarization properties

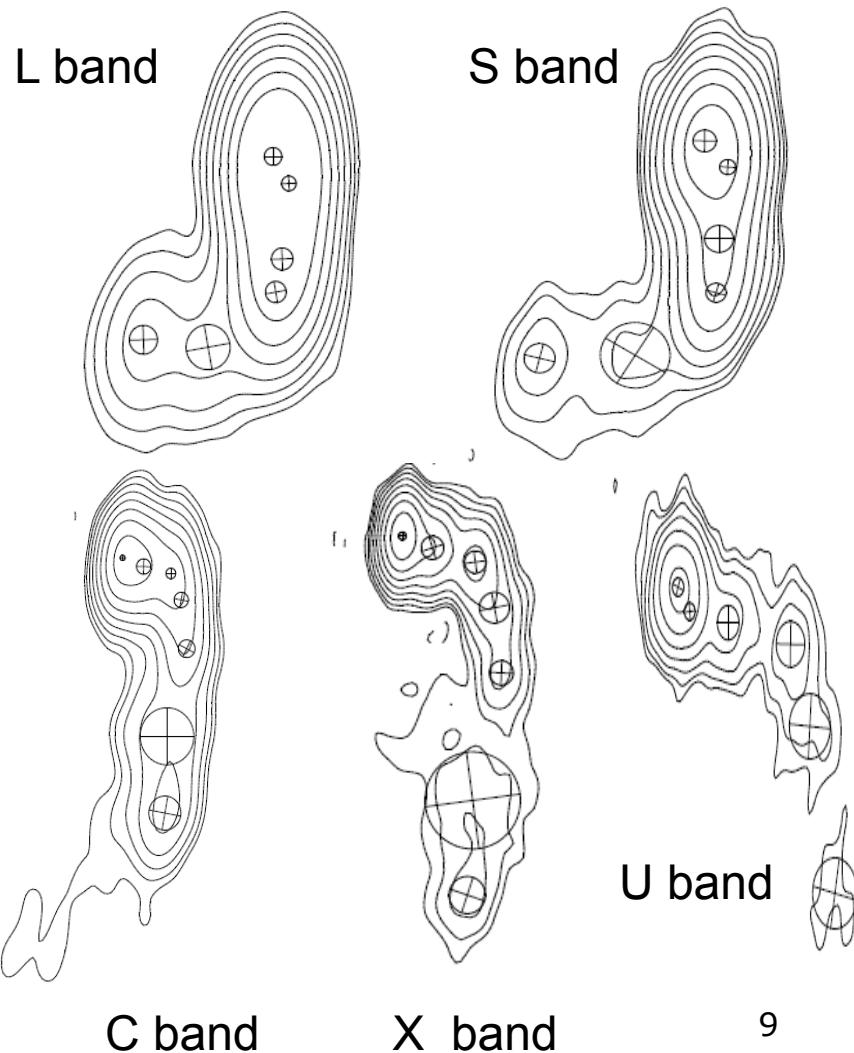


Model fitting

Table 2. Component parameters in OQ172

Frequency	Comp.	Flux (Jy)	R (mas)	θ (deg)	Major (mas)	T_B ($10^{10}K$)
1.6 GHz	Core	0.766 ± 0.074	0.00	...	1.93	69.78
	L5	0.492 ± 0.064	3.38 ± 0.04	-148	1.60	63.56
	L4	0.381 ± 0.053	11.06 ± 0.09	-174	2.37	22.43
	L3	0.174 ± 0.041	14.58 ± 0.10	-178	2.29	10.97
	L2	0.054 ± 0.020	21.71 ± 0.74	-199	4.85	0.76
	L1	0.054 ± 0.020	24.34 ± 0.43	-215	3.10	1.86
2.2 GHz	Core	0.859 ± 0.081	0.00	...	2.02	33.12
	S5	0.382 ± 0.058	3.12 ± 0.05	-140	1.40	31.39
	S4	0.236 ± 0.044	9.12 ± 0.14	-172	2.50	6.08
	S3	0.207 ± 0.041	14.04 ± 0.11	-175	1.75	10.89
	S2	0.042 ± 0.025	20.68 ± 1.65	-196	6.05	0.18
	S1	0.031 ± 0.017	24.65 ± 0.60	-215	2.70	0.68
4.8 GHz	Core	0.256 ± 0.029	0.00	...	0.30	96.75
	C6	0.234 ± 0.028	1.38 ± 0.03	-111	0.88	10.28
	C5	0.117 ± 0.020	3.08 ± 0.03	-106	0.60	11.05
	C4	0.077 ± 0.017	4.32 ± 0.05	-123	0.87	3.46
	C3	0.054 ± 0.014	6.53 ± 0.08	-143	1.02	1.77
	C2	0.067 ± 0.019	10.62 ± 0.45	-165	3.29	0.21
	C1	0.054 ± 0.014	14.91 ± 0.22	-170	1.96	0.48
8.3 GHz	Core	0.304 ± 0.028	0.00	...	0.31	36.67
	X6	0.124 ± 0.019	1.32 ± 0.05	-111	0.93	1.66
	X5	0.074 ± 0.014	3.18 ± 0.07	-109	0.89	1.08
	X4	0.032 ± 0.010	4.76 ± 0.16	-127	1.24	0.24
	X3	0.019 ± 0.008	6.86 ± 0.16	-143	0.98	0.23
	X2	0.039 ± 0.025	11.05 ± 1.27	-164	3.92	0.03
	X1	0.016 ± 0.008	14.72 ± 0.34	-169	1.49	0.08
	Core	0.181 ± 0.025	0.00	...	0.30	6.85
15.3 GHz	U7	0.036 ± 0.013	$.51 \pm 0.02$	-142	0.29	1.46
	U6	0.035 ± 0.012	1.47 ± 0.08	-114	0.58	0.35
	U5	0.024 ± 0.011	3.18 ± 0.16	-107	0.77	0.14
	U4	0.013 ± 0.010	4.27 ± 0.42	-123	1.10	0.04
	U3	0.008 ± 0.010	6.70 ± 0.76	-140	1.20	0.02

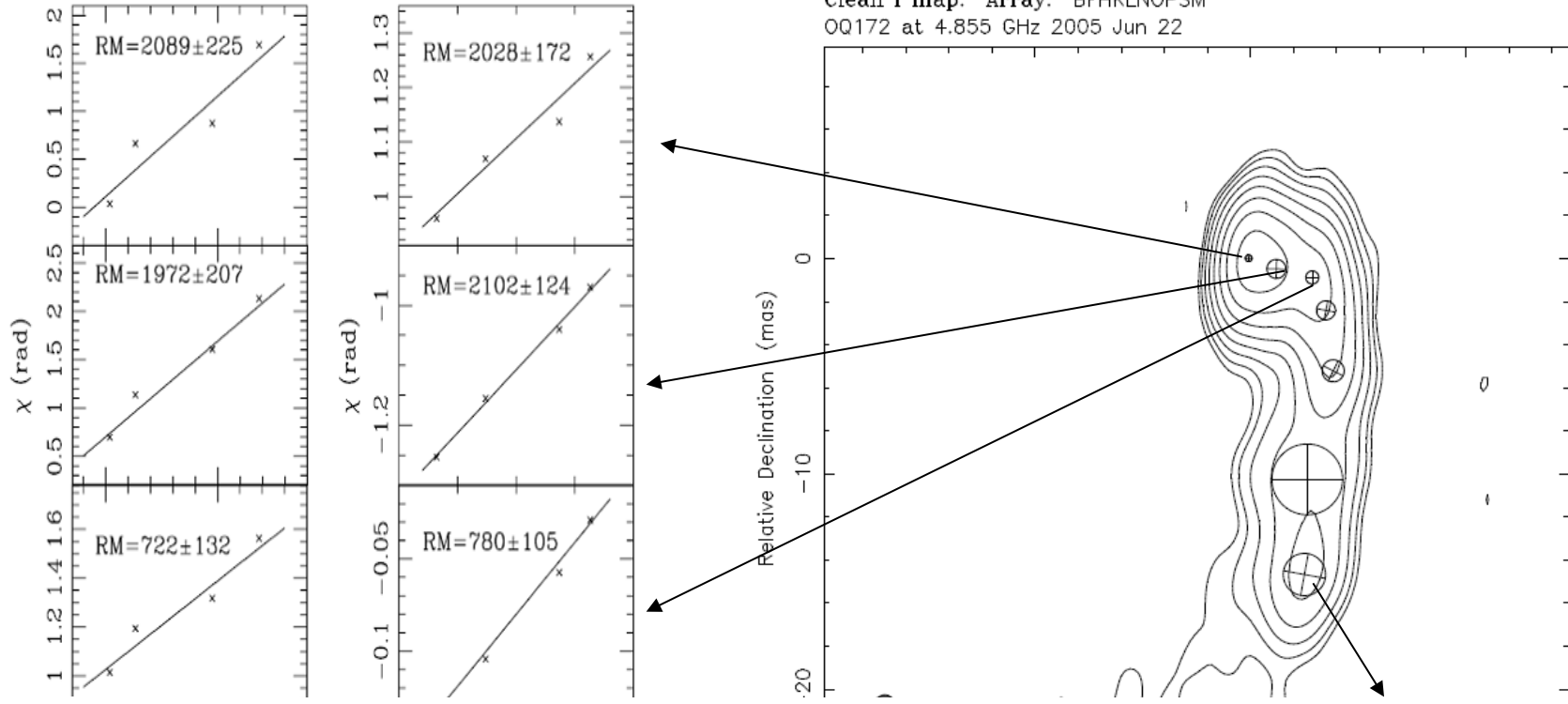
Note: Column (1): Observing frequency. Column (2): Component name. Column (3): Total flux density of each c
 Column (4): Distance of each component from the core. Column (5): Position angle of each component. Column
 axis of each component. Column (7): the bright temperature of each component in unit of $10^{10}K$.





Rotation Measure at Inner Jet

Clean I map. Array: BFHKLNOPSM
OQ172 at 4.855 GHz 2005 Jun 22



The GPS source has an intrinsic property of small size, which could be due to their young age or dense environment constraining their size. OQ172 has an extremely high rest-frame rotation measure in core and inner jet region which indicate there are abundant dense gas surrounding the projected region about 90 pc.

Fig. 2.-
band.

1

ty
al
f
in





SSA and FFA fitting

GPS sources are characterized by their compact overall size (< 1 kpc) and convex radio spectrum peaked at GHz frequency (O'Dea et al. 1991). This convex radio spectrum is possible caused by synchrotron self-absorption or free-free absorption (O'Dea 1998). Our simultaneous multi-frequency VLBA observation would give us a chance to further investigate absorption phenomenon in GPS quasar OQ172.

SSA:
$$S_\nu = S_0 \nu^\alpha \exp(-\tau_f \nu^{-2.1}),$$

FFA:
$$S_\nu = S_0 \nu^{2.5} [1 - \exp(-\tau_s \nu^{\alpha-2.5})],$$

where τ_s and τ_f are the SSA and FFA coefficient respectively, S_0 , ν and α are the flux density at 1 GHz, the frequency in GHz, and the spectra index.

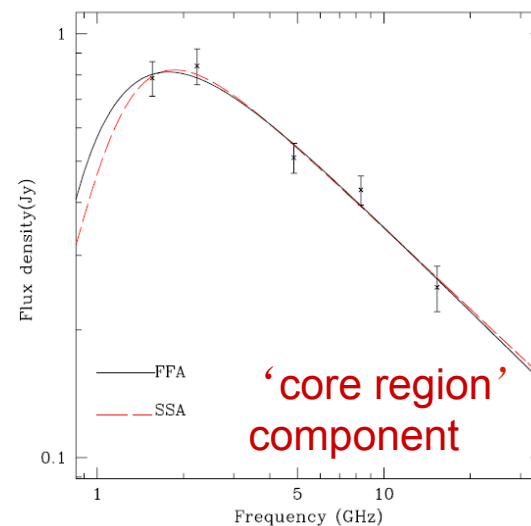


Fig. 4.— Spectra of the 'core' component (see text) at our multi-frequency observation. The solid and dashed lines indicate the fitted spectra for the FFA and SSA models, respectively.

Table 4. Spectral fit for synchrotron self-absorption (SSA) and free-free absorption (FFA).

Model	S_0 (Jy)	τ_s	χ^2	Model	S_0 (Jy)	τ_f	χ^2
SSA	0.25 ± 0.04	13.8 ± 2.9	2.32	FFA	1.63 ± 0.5	1.1 ± 0.4	2.53

Note: Column (1): SSA model. Column (2): S_0 in Jy. Column (3): SSA coefficient. Column (4): χ^2 for SSA fitting. Column (5): FFA model. Column (6): S_0 in Jy. Column (7): FFA coefficient. Column (8): χ^2 for FFA fitting.

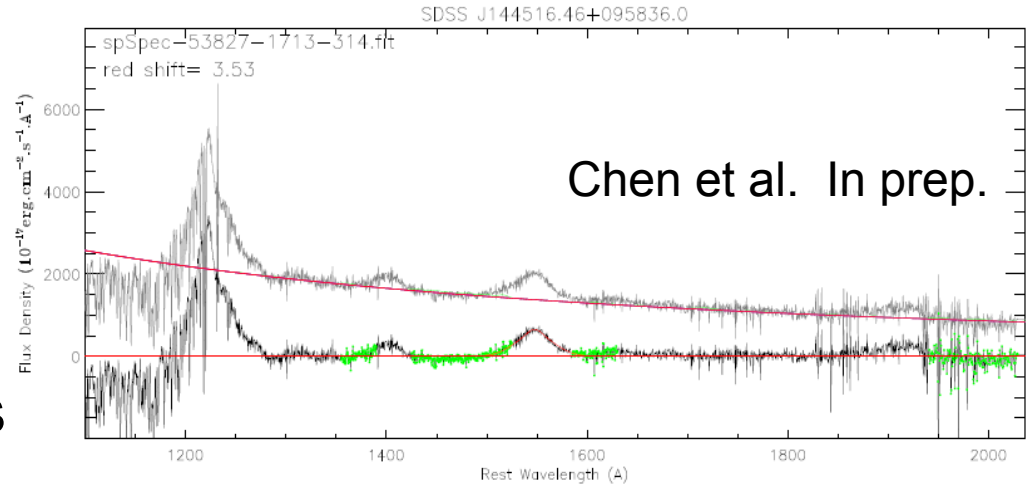
SSA: $\nu_{\max} \sim 8B^{1/5} S_m^{2/5} \theta^{-4/5} (1+z)^{1/5}$ GHz, $\implies B = 3.45$ mG

FFA+RM: $\tau_v = 0.08235 \nu^{-2.1} \int T_e^{-1.35} N_e^2 dl$,
 $RM = 812 \int_0^L n_e B_{\parallel} dl$ rad m⁻², \implies if $T = 10^4$ K, $L = 40$ pc (30°),
then $n_e = 2.617 \times 10^3$ cm⁻³, $B = 0.15$ mG



Black Hole Mass and Jet Power

SDSS DR8
 FWHM=8848km/s
 EW=18.8 Å
 L_CIV=1.44*e45 ergs/s



$$M_{\text{BH}}(\text{C IV}) = 4.6 \times 10^5 \left(\frac{L(\text{C IV})}{10^{42} \text{ erg s}^{-1}} \right)^{0.60 \pm 0.16} \left(\frac{\text{FWHM}(\text{C IV})}{1000 \text{ km s}^{-1}} \right)^2 M_{\odot}$$

$$\log M_{\text{BH}} = 9.45 M_{\odot}$$

$$\log m = -1.46$$

$$\log L_{\text{bol}} = 46.1 \text{ ergs s}^{-1}$$

$$\log Q_{\text{jet}} = 46.95 \text{ ergs s}^{-1}$$

$Q_{\text{jet}} > L_{\text{bol}} \implies$ require an intense accretion flow



CONCLUSIONS

- ◆ A core-jet structure has been imaged from all five frequencies observation, and a sharp large bending at ~ 3 mas far away from core can be clearly found at C, X, and U band. Comparing to previous observation, a new component was identified at C band.
- ◆ Linear polarization has been detected in OQ172 at all five bands. The depolarized effect exists on two low bands. At C and X band, we could linear fit the faraday rotation in core and inner jet parts. The value of the RM is large about $\gg 2000$ rad m^{-2} in core components and about $\gg 700$ rad m^{-2} in inner jet part. The rotation measure varies along with the jet and goes down low value at outer jet parts.
- ◆ Our simultaneous multi-frequency VLBA observation can be used to investigate absorption phenomenon in GPS quasar OQ172. To investigate the low frequency cut off radio spectrum in core region component in OQ172, we use both SSA and FFA fitting for its flux density. And based on fitting results some physical parameters can be derived in OQ172.
- ◆ We also calculated the massive black hole mass and the jet power of OQ172. The large width for $[OIII]_{5007}$ in OQ172 might not due to the center massive black hole, but to other physical reasons, such as the interaction between jet and narrow line region.



Thanks !!